Lysine acetylation restricts mutant IDH2 activity to optimize transformation in AML cells
Dong Chen, et al.

SUPPLEMENTAL INFORMATION

Supplemental Data (Figure S1-S5)

Figure S1

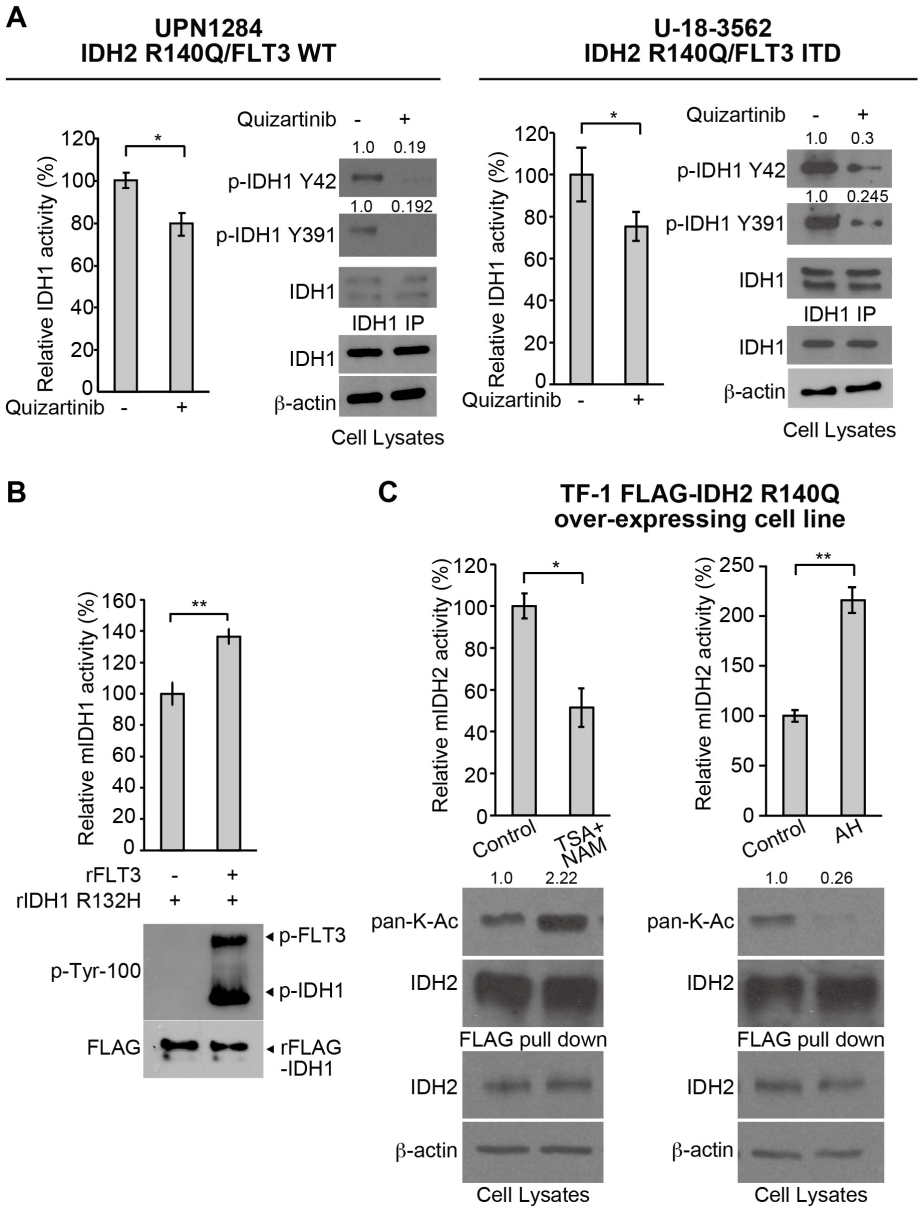

Figure S1, Related to Figure 1

FLT3 regulates mIDH2 activity by controlling lysine acetylation.

(A) Human primary AML cells expressing mIDH2 were treated with FLT3 inhibitor quizartinib, followed by IDH1 enzyme activity assay (*left* panels) and immunoprecipitation (IDH1 IP) prior to Western blotting to detect Y42- and Y391-phosphrylation levels of endogenous IDH1.
(B) Purified recombinant IDH1 R132H protein was incubated with recombinant active form of rFLT3 in an *in vitro* kinase assay, followed by mIDH1 enzyme activity assay (*upper*); tyrosine phosphorylation of mIDH1 was detected by Western blotting (*lower*).
(C) TF-1 erythroleukemia cells expressing IDH2 R140Q mutant were treated with or without NAM/TSA (*left*) or ACAT1 inhibitor arecoline AH (*right*), followed by mIDH2 enzyme activity assay (*upper* panels); lysine acetylation of mIDH2 was detected by Western blotting (*lower* panels).
The error bars represent mean values ±SD from three replicates of each sample (*: 0.01<p<0.05; **: 0.01<p<0.001); Data are mean ±SD; p values were obtained by a two-tailed Student's t-test.

Figure S2

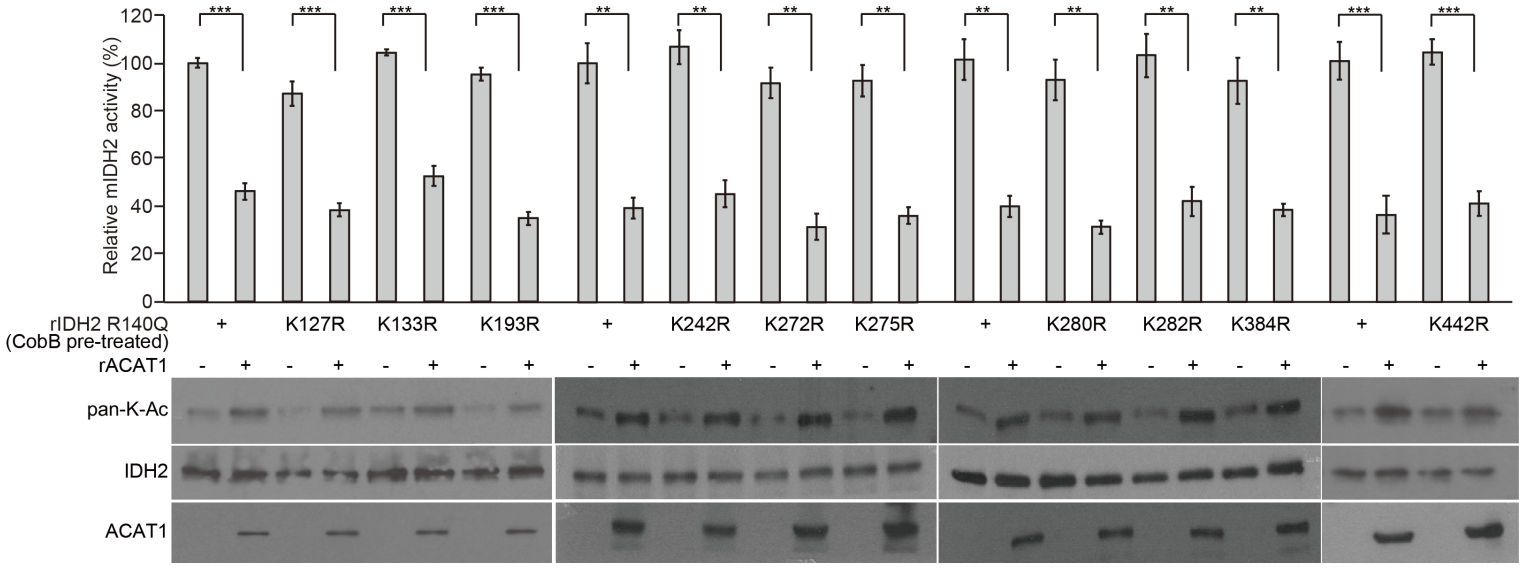

Figure S2, Related to Figure 1

K413-acetylation inhibits IDH2 enzyme activity. Purified IDH2 R140Q variants with representative individual K→R mutation were pre-treated with cobB prior to incubation with acetyltransferase rACAT1, followed by mIDH2 catalytic activity assay (*upper*) and Western blot to detect lysine acetylation (*lower*).
The error bars represent mean values ±SD from three replicates of each sample (**: 0.01<p<0.001; ***: p<0.001; ns: not significant); Data are mean ± SD; p values were obtained by a two-tailed Student's t-test.

Figure S3

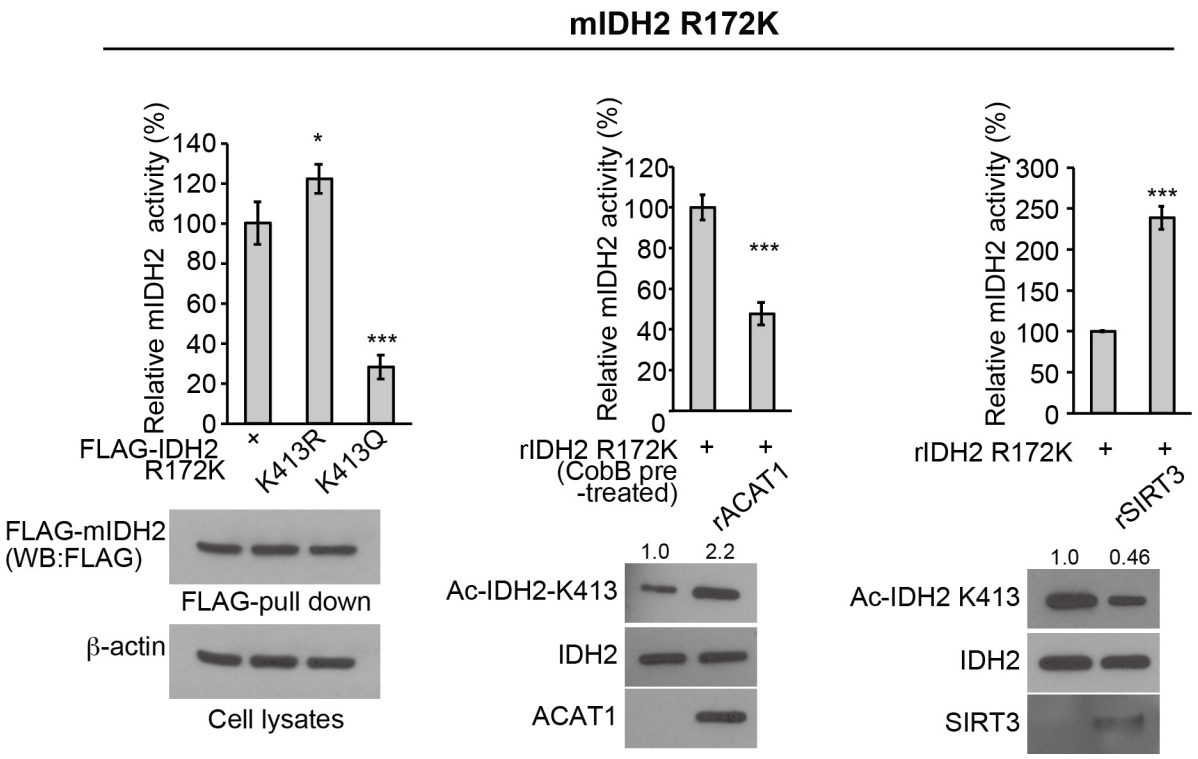

Figure S3, Related to Figure 2

K413-acetylation inhibits IDH2 R172K mutant with ACAT1 and SIRT3 as upstream acetyltransferase and deacetylase, respectively. *Left*: FLAG-IDH2 R172K variants were overexpressed in 293T cells and FLAG-pull down samples were applied to mIDH2 activity assay and Western blot. Middle-right: Purified IDH2 R172K protein was either pre-treated with cob followed by incubation with upstream acetyltransferase rACAT1 (*middle*) or incubated with deacetylase SIRT3 (*right*), followed by mIDH2 catalytic activity assay and Western blot to detect K413 acetylation.
The error bars represent mean values ±SD from three replicates of each sample (***: $p<0.001$); Data are mean ± SD; p values were obtained by a two-tailed Student's t-test.

Figure S4

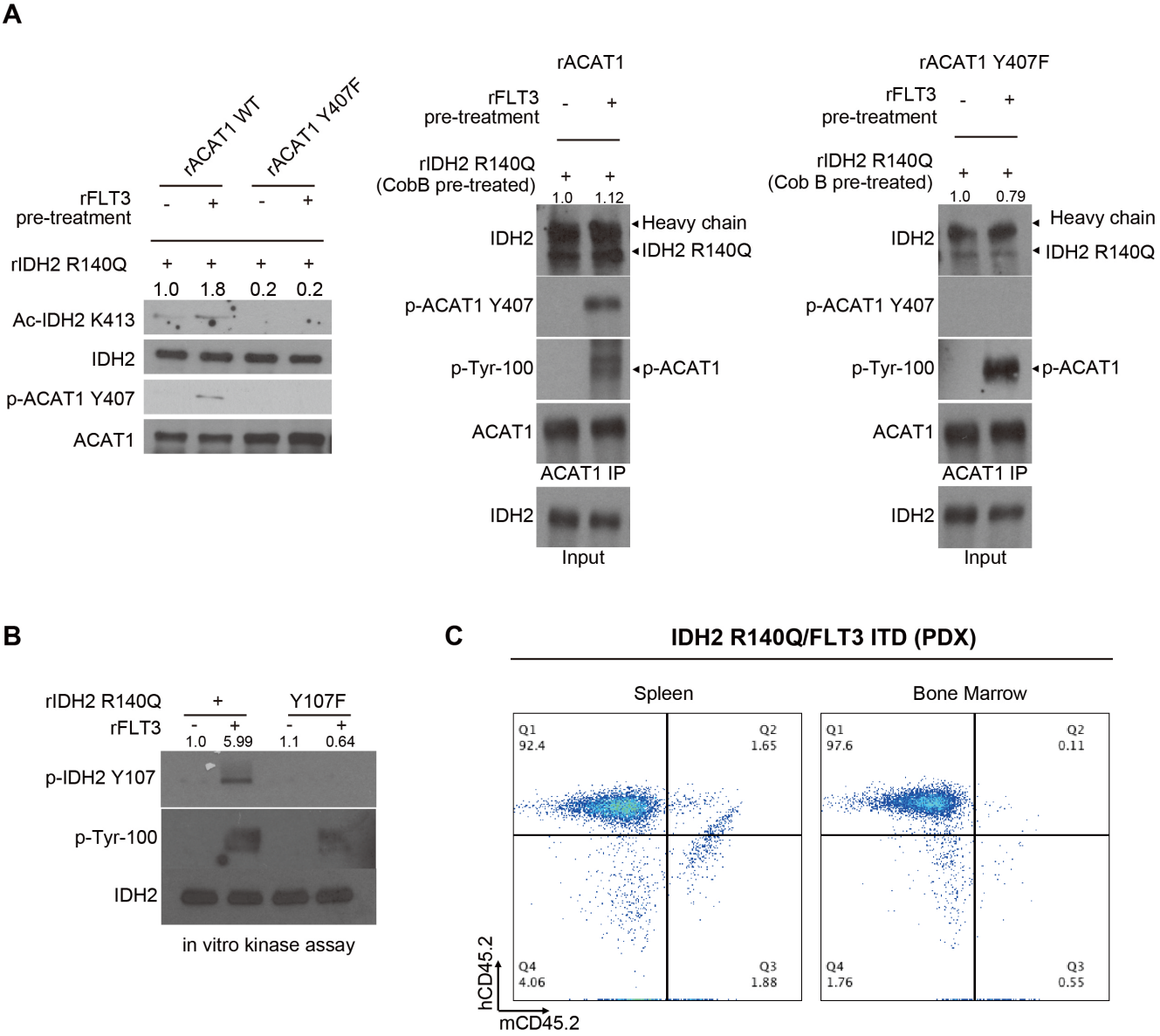

Figure S4, Related to Figure 4

Y107-phosphorylation of IDH2 by FLT3 promotes ACAT1 binding.
(A) *Left*: Purified ACAT1 WT or Y407 mutant proteins were incubated with or without purified FLT3, followed by an *in vitro* ACAT1 acetyltransferase assay using purified IDH2 R140Q mutant as an exogenous substrate. Western blot was performed to assess K413 acetylation of mutant IDH2. Purified rACAT1 (*middle*) and rACAT1 Y407F mutant (*right*) proteins were pre-treated with rFLT3, followed by incubation with rIDH2 R140Q proteins pre-treated with cobB, prior to ACAT1 IP and Western blotting to detect co-immunoprecipitated IDH2 R140Q and Y407-phosphorylation of ACAT1.

(B) Western blotting results using purified specific phosphor-IDH2 antibody (p-Y107) to detect Y107-phosphorylation of rIDH2 R140Q and control Y107F mutant proteins by FLT3 in an *in vitro* kinase assay.
(C) Engraftment of leukemia cells expressing IDH2 R140Q and FLT3 ITD mutants from an AML patient into NSG mice is shown. Infiltration of AML cells in spleen (92.4%) and bone marrow (97.6%) in PDX mice was assessed by staining single cells with anti-human CD45 (hCD45) at week 15 after xenograft.

Figure S5

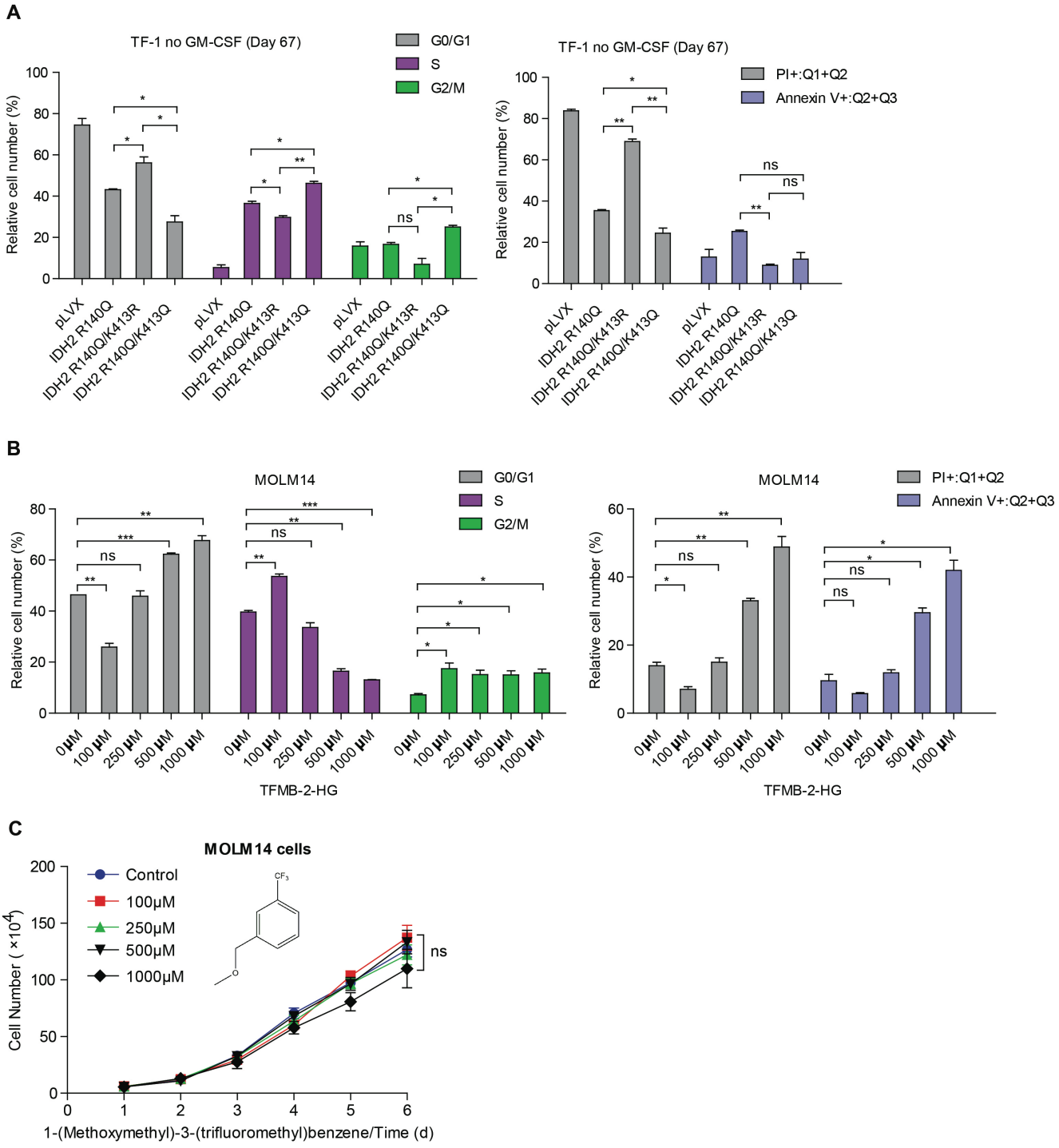

Figure S5, Related to Figure 5

Effects of intracellular 2-HG on cell cycle and cell death.

(A-B) Results of quantitation and statistical analysis of two independent biological replicates are shown in Figure 5D (A) and Figure 5G (B).
(C) MOLM14 cells were treated with increasing concentrations up to 1,000 μM of 1-(Methoxymethyl)-3-(trifluoromethyl)benzene for 6 days. Cell proliferation was assessed by daily counting of cells.
The error bars represent mean values ±SD from two independent biological replicates of each sample (*: $0.01<p<0.05$; **: $0.01<p<0.001$; ***: $p<0.001$; ns: not significant); Data are mean ± SD; p values were obtained by a two-tailed Student's t-test.